Tokyo Climate Center, Japan Meteorological Agency

TCC News

No. 36 Spring 2014

Contents Page

El Niño Outlook (April – October 2014)

It is likely that El Niño conditions will develop during the Northern Hemisphere summer.

El Niño/La Niña

In March 2014, the NINO.3 SST was near normal with a deviation of -0.1°C, and SSTs (Figures 1 and 3 (a)) were above normal in the western equatorial Pacific. Subsurface temperatures (Figures 2 and 3 (b)) were above normal in most regions from the western to the eastern equatorial Pacific, while zonal winds in the lower troposphere were near normal over the central equatorial Pacific. These oceanic and atmospheric observations indicate that ENSO-neutral conditions continued in the equatorial Pacific.

According to JMA's El Niño prediction model, the NINO.3 SST will be above normal during the Northern Hemisphere summer and beyond (Figure 4). It is considered that the eastward migration of warm waters as observed throughout the equatorial Pacific will cause SST anomalies to increase in its eastern part. In conclusion, the NINO.3 SST is likely to turn from near normal to above normal in the months ahead, and it is likely that El Niño conditions will develop during the Northern Hemisphere summer.

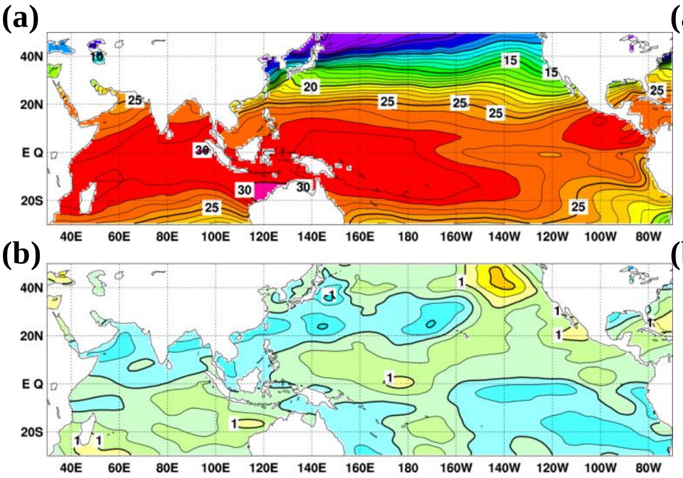

Figure 1 Monthly mean (a) sea surface temperatures (SSTs) and (b) SST anomalies in the Indian and Pacific Ocean areas for March 2014
The contour intervals are 1˚C in (a) and 0.5˚C in (b). The base period for the normal is 1981 – 2010.

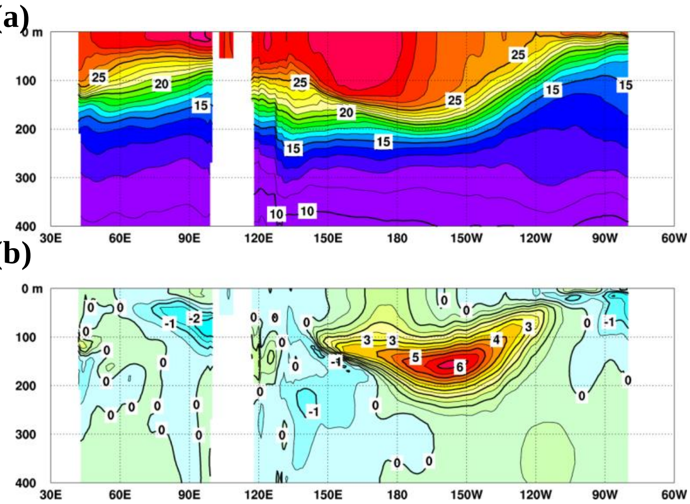

Figure 2 Monthly mean depth-longitude cross sections of (a) temperatures and (b) temperature anomalies in the equatorial Indian and Pacific Ocean areas for March 2014
The contour intervals are 1˚C in (a) and 0.5˚C in (b). The base period for the normal is 1981 – 2010.

Western Pacific and Indian Ocean

The area-averaged SST for the tropical western Pacific (NINO.WEST) region was near normal in March, and is likely to be near normal in the Northern Hemisphere spring and near or below normal in summer.

The area-averaged SST for the tropical Indian Ocean basin-wide (IOBW) region was near normal in March, and is likely to be near normal in the Northern Hemisphere spring and summer.

(Ichiro Ishikawa, Climate Prediction Division)

* The SST normal for NINO.3 region (5°S – 5°N, 150°W – 90°W) is defined as an monthly average over a sliding 30-year period (1984 – 2013 for this year).

* The SST normals for the NINO.WEST region (Eq. – 15°N, 130°E – 150°E) and the IOBW region (20°S – 20°N, 40°E – 100°E) are defined as linear extrapolations with respect to a sliding 30-year period in order to remove the effects of significant long-term warming trends observed in these regions.

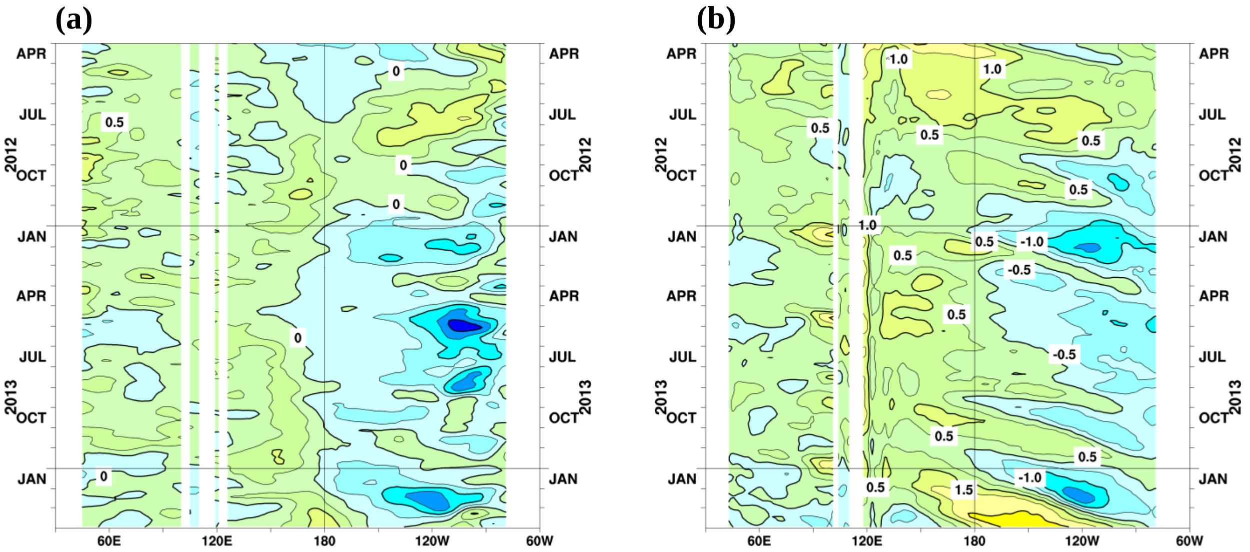

Figure 3 Time-longitude cross sections of (a) SST and (b) ocean heat content (OHC) anomalies along the equator in the Indian and Pacific Ocean areas

OHCs are defined here as vertical averaged temperatures in the top 300 m. The base period for the normal is 1981 – 2010.

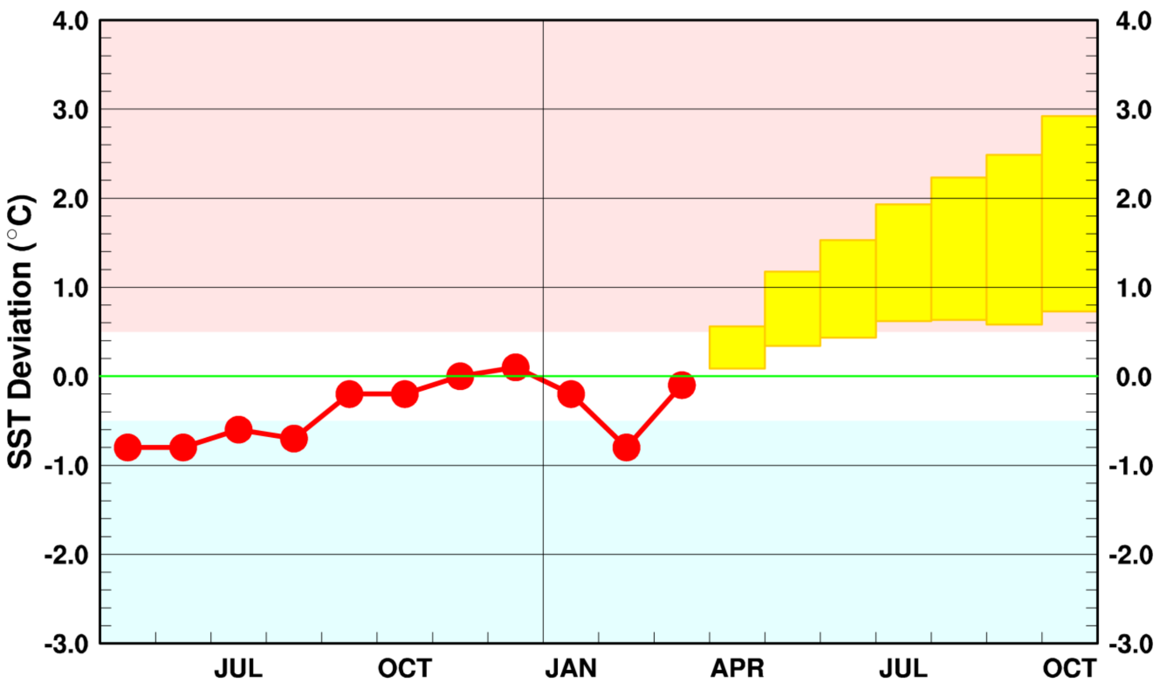

Figure 4 Outlook of NINO.3 SST deviation produced by the El Niño prediction model

This figure shows a time series of monthly NINO.3 SST deviations. The thick line with closed circles shows observed SST deviations, and the boxes show the values produced for the next six months by the El Niño prediction model. Each box denotes the range into which the SST deviation is expected to fall with a probability of 70%.

Based on JMA's seasonal ensemble prediction system, sea surface temperature (SST) anomalies in the eastern equatorial Pacific Ocean will be above normal this boreal summer, suggesting a very likely transition to El Niño conditions. In line with this prediction, active convection over the eastern part of the Pacific and a southward shift of the sub-tropical jet stream are expected. Conversely, inactive convection is predicted over the Maritime Continent and the northern part of the Indian Ocean.

1. Introduction

This article outlines JMA's dynamical seasonal ensemble prediction for boreal summer 2014 (June – August, referred to as JJA), which was used as a basis for the Agency's operational warm-season outlook issued on 25 April 2014. The outlook detailed here is based on the seasonal ensemble prediction system of the Coupled atmosphere-ocean General Circulation Model (CGCM). See the column below for system details.

Section 2 outlines global SST anomaly predictions, and Section 3 describes the associated circulation fields expected over the tropics and sub-tropics. Finally, the circulation fields predicted for the mid- and high latitudes of the Northern Hemisphere are discussed in Section 4.

2. SST anomalies (Figure 5)

Figure 5 shows predicted SSTs and related anomalies for JJA. Anomalies in the central equatorial Pacific Ocean are above normal throughout the period, suggesting a very likely transition to El Niño conditions. Conversely, SST anomalies are slightly below normal around the Philippines. They are also expected to be near normal in the northern part of the Indian Ocean but slightly above normal in its southern part.

3. Prediction for the tropics and sub-tropics (Figure 6)

Figure 6 (a) shows predicted precipitation and related anomalies for JJA. In association with the expected El Niño conditions, precipitation amounts around the central equatorial Pacific Ocean are expected to be above normal. Conversely, those around the Maritime Continent and the northern part of the Indian Ocean are expected to be below normal.

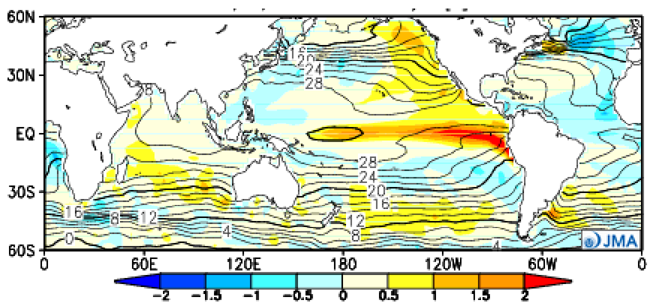

Figure 5 Predicted SSTs (contours) and SST anomalies (shading) for June – August 2014 (ensemble mean of 51 members)

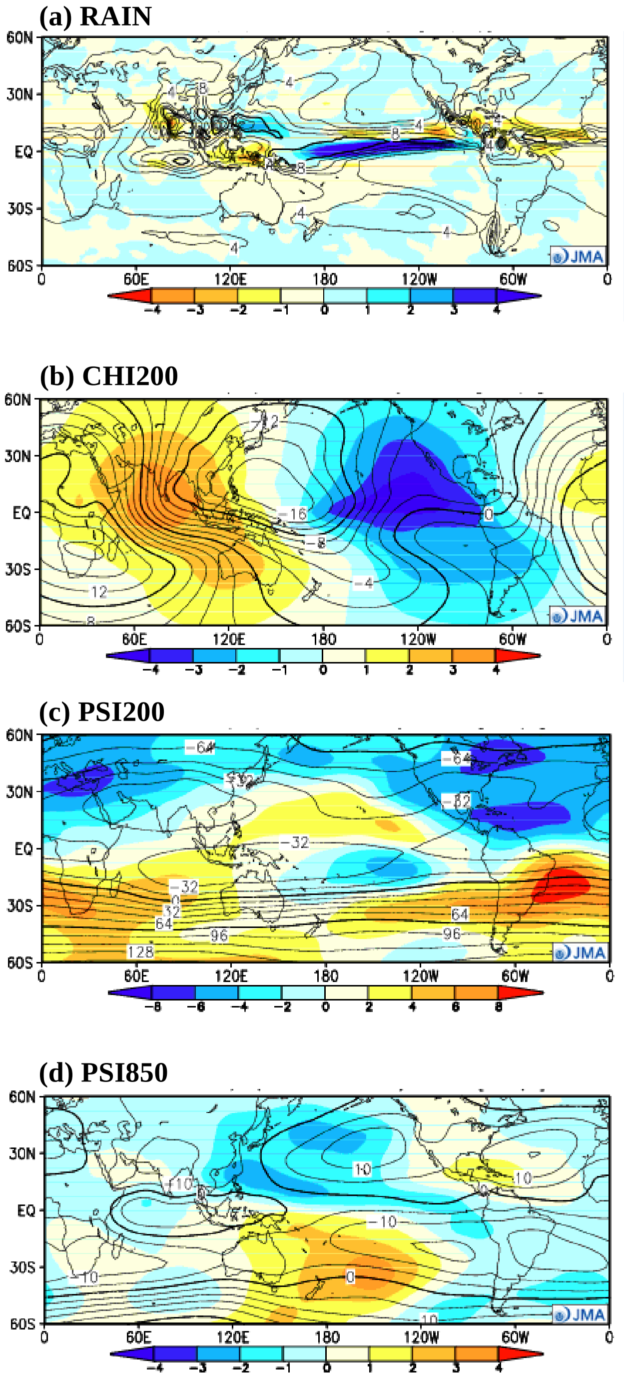

Figure 6 Predicted atmospheric fields from 60°N – 60°S for June – August 2014 (ensemble mean of 51 members)
(a) Precipitation (contours) and anomaly (shading). The contour interval is 2 mm/day.
(b) Velocity potential at 200 hPa (contours) and anomaly (shading). The contour interval is 2 × 106 m2/s.
(c) Stream function at 200 hPa (contours) and anomaly (shading). The contour interval is 16 × 106 m2/s.
(d) Stream function at 850 hPa (contours) and anomaly (shading). The contour interval is 5 × 106 m2/s.

Velocity potential in the upper troposphere (200 hPa) (Figure 6 (b)) is expected to be negative (i.e., more divergent) over the eastern part of the Pacific, reflecting active convection over the central equatorial part of the Pacific Ocean. Conversely, positive (i.e., more convergent) anomalies are expected around the Maritime Continent and the northern part of the Indian Ocean, reflecting inactive convection in these regions.

The stream function at 200 hPa (Figure 6 (c)) is expected to be zonally negative (i.e., cyclonic) in the mid- and high latitudes of the Northern Hemisphere, indicating a southward-shifting tendency for the subtropical jet stream. Positive (i.e., anti-cyclonic) anomalies are expected to the east of the Philippines, reflecting above-normal precipitation in the region.

The stream function at 850 hPa (Figure 6 (d)) is expected to exhibit negative (i.e., cyclonic) anomalies to the east of the Philippines, suggesting development of the monsoon trough in the region.

4. Prediction for the mid- and high latitudes of the Northern Hemisphere (Figure 7)

Geo-potential height anomalies at 500 hPa (Figure 7 (a)) are expected to be positive over most of the Northern Hemisphere, reflecting the influence of the recent warming trend. However, the North Pacific is expected to exhibit clear negative anomalies, which may be related to the southward-shifting tendency of the subtropical jet stream.

Negative anomalies of sea level pressure (Figure 7 (b)) are expected in most regions of the North Pacific, suggesting a diminished North Pacific High.

(Takashi Yamada, Climate Prediction Division)

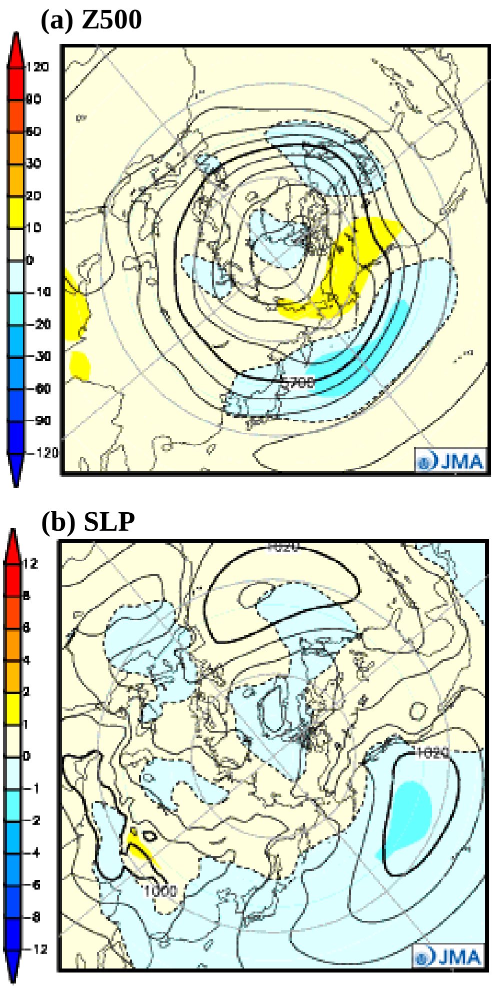

Figures 7 Predicted atmospheric fields from 20°N – 90°N for June – August 2014 (ensemble mean of 51 members)
(a) Geopotential height at 500 hPa (contours) and anomaly (shading). The contour interval is 60 m.
(b) Sea level pressure (contours) and anomaly (shading). The contour interval is 4 hPa.

JMA's Seasonal Ensemble Prediction System

JMA operates a seasonal Ensemble Prediction System (EPS) using the Coupled atmosphere-ocean General Circulation Model (CGCM) to make seasonal predictions beyond a one-month time range. The EPS produces perturbed initial conditions by means of a combination of the initial perturbation method and the lagged average forecasting (LAF) method. The prediction is made using 51 members from the latest six initial dates (nine members are run every five days). Details of the prediction system and verification maps based on 30-year hindcast experiments (1979 – 2008) are available at http://ds.data.jma.go.jp/tcc/tcc/products/model/.

Warm Season Outlook for Summer 2014 in Japan

In summer 2014, mean temperatures are expected to be either near or below normal (both with 40% probability) in northern Japan and either near or above normal (both with 40% probability) in western Japan and Okinawa/Amami. Total summer precipitation amounts are expected to be either near or above normal (both with 40% probability) in northern Japan, and either near or below normal (both with 40% probability) in western Japan.

1. Outlook summary

JMA issued its outlook for the coming summer over Japan in February and updated it in March and April. In summer (June – August) 2014, mean temperatures are expected to be either near or below normal (both with 40% probability) in northern Japan, and either near or above normal (both with 40% probability) in western Japan and Okinawa/Amami. Summer total precipitation amounts are expected to be either near or above normal (both with 40% probability) in northern Japan, and either near or below normal (both with 40% probability) in western Japan (Figure 8). Rainy season (Baiu) precipitation amounts are unlikely to exhibit particular characteristics in any region.

2. Outlook background

JMA's coupled global circulation model predicts that the NINO.3 SST will transition from near to above normal in summer. In conclusion, although the continuation of ENSO-neutral conditions may be possible considering the large uncertainties of the model's prediction, it is more likely that El Niño conditions will develop.

In association with these SST anomalies, atmospheric convection is predicted to be more active than normal over the central and eastern tropical Pacific and less active than normal from the eastern Indian Ocean to the Maritime Continent. In connection with this relatively inactive convection, the Tibetan High is predicted to be weaker than normal. The subtropical jet, which flows along the northern edge of the Tibetan High, is likely to shift southward from its normal position. Meanwhile, convection is predicted to be more active than normal around the Philippines in relation to inactive convection occurring from the eastern Indian Ocean to the Maritime Continent. As a result, the North Pacific high is expected to be weaker than normal over northern Japan and stronger than normal over western Japan and Okinawa/Amami.

The tropospheric thickness temperature averaged over the mid-latitudes of the Northern Hemisphere (30°N – 50°N), which correlates to temperatures over Japan, is predicted to be around normal.

(Masayuki Hirai, Climate Prediction Division)

Temperature

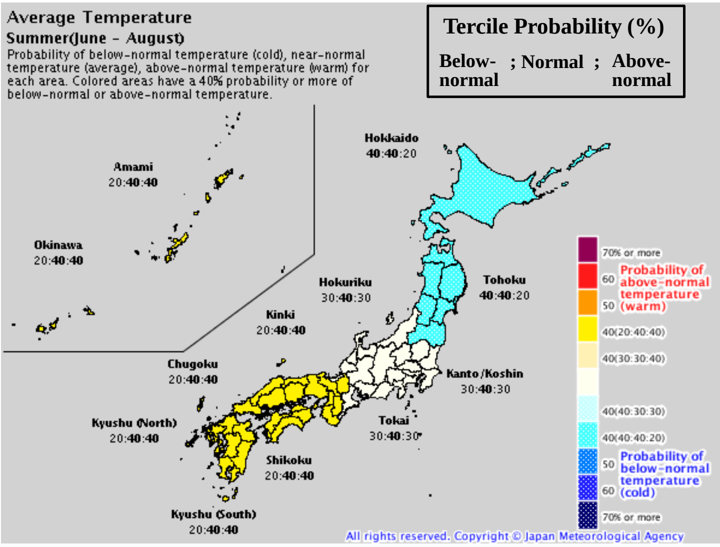

Precipitation

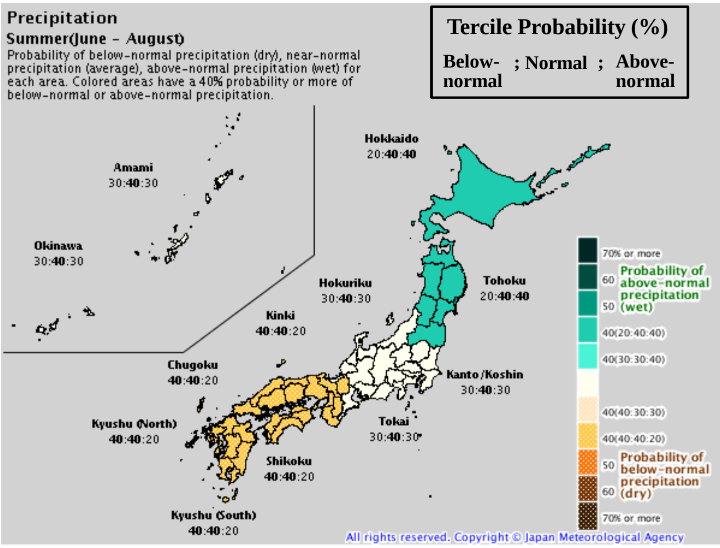

Figure 8 Outlook for summer 2014 temperature (above) and precipitation (below) probabilities in Japan

Summary of the 2013/2014 Asian Winter Monsoon

This report summarizes the characteristics of the surface climate and atmospheric/oceanographic considerations related to the Asian winter monsoon for 2013/2014.

Note: Japanese 55-year Reanalysis (JRA-55; http://jra.kishou.go.jp/JRA-55/index_en.html) atmospheric circulation data and COBE-SST (JMA 2006) sea surface temperature (SST) data were used for this investigation. The outgoing longwave radiation (OLR) data referenced to infer tropical convective activity were originally provided by NOAA. The base period for the normal is 1981 – 2010. The term "anomaly" as used in this report refers to deviation from the normal.

1. Surface climate conditions

1.1 Overview of Asia

In boreal winter 2013/2014, temperatures were above or near normal in many parts of East Asia and in eastern Siberia, and were below normal in many parts of South, Southeast and Central Asia (Figure 9). Very high or low temperatures were recorded on a regional scale in December, January and February, but were not seen on this scale in the three-month mean field.

Figure 10 shows extreme climate events observed from December 2013 to February 2014. In December, extremely high temperatures were observed in Mongolia and Siberia, and extremely low temperatures were recorded on the Indochina Peninsula and in southern China. Extremely heavy precipitation amounts were observed over parts of Southeast Asia. In January, extremely high temperatures were seen in Mongolia and in northern and eastern China, while extremely low temperatures were seen around the South China Sea. In February, extremely low temperatures were observed in Central Asia and the eastern Middle East. Extremely heavy precipitation amounts were observed in parts of Japan, and extremely light precipitation amounts were seen in parts of Indonesia and on the Malay Peninsula.

Figure 11 shows time-series representations of daily temperatures at Bangkok in Thailand and Astana in Kazakhstan for winter 2013/2014. Daily mean temperatures were below normal in the second halves of December and January and near normal for other parts of winter at Bangkok. Daily mean temperatures were above normal on many days in December and below normal on most days from the second half of January to the end of February at Astana.

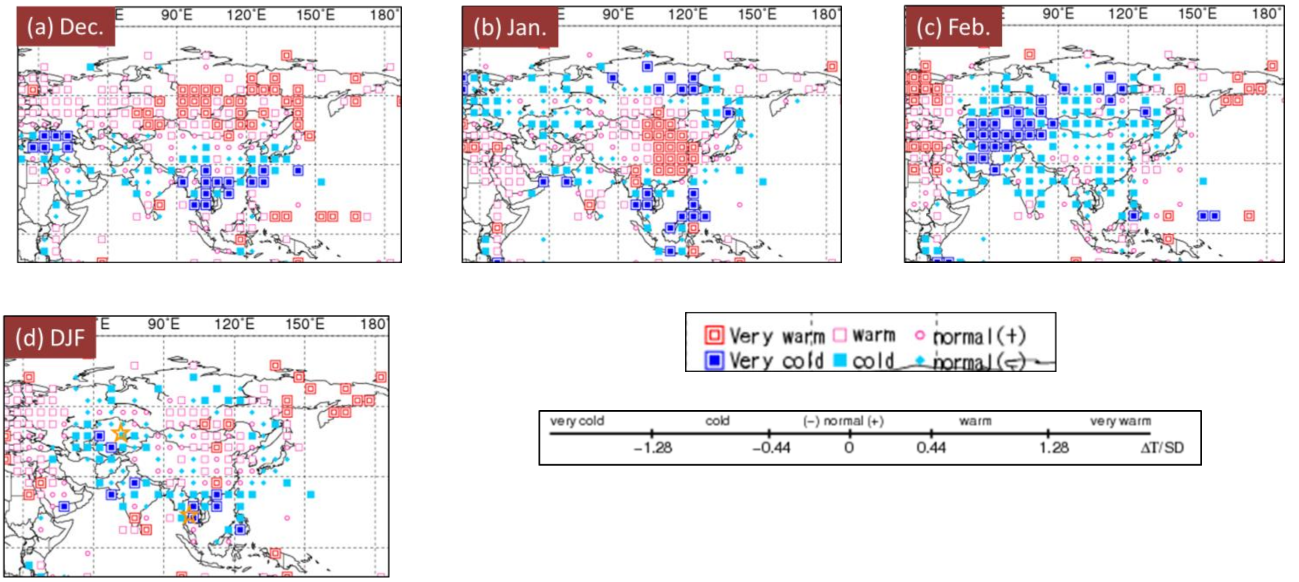

Figure 9 Monthly mean temperature anomalies for (a) December 2013, (b) January 2014 and (c) February 2014, and (d) three-month mean temperature anomalies for December 2013 – February 2014

Categories are defined by the monthly/three-month mean temperature anomaly against the normal divided by its standard deviation and averaged in 5° × 5° grid boxes. The thresholds of each category are -1.28, -0.44, 0, +0.44 and +1.28. Standard deviations were calculated from 1981 – 2010 statistics. Areas over land without graphical marks are those where observation data are insufficient or where normal data are unavailable. In (d), the orange stars indicate the locations of Bangkok (Thailand) and Astana (Kazakhstan). Daily temperature data for both cities are shown in Figure 11.

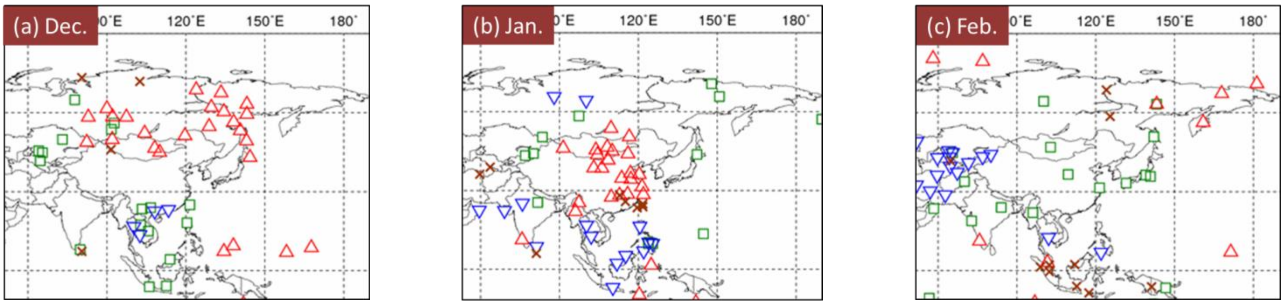

Figure 10 Extreme climate events for (a) December 2013, (b) January 2014 and (c) February 2014

△ Extremely high temperature (ΔT/SD > 1.83) □ Extremely heavy precipitation (Rd = 6)

▽ Extremely low temperature (ΔT/SD < -1.83) × Extremely light precipitation (Rd = 0)

ΔT, SD and Rd indicate temperature anomaly, standard deviation and quintile, respectively.

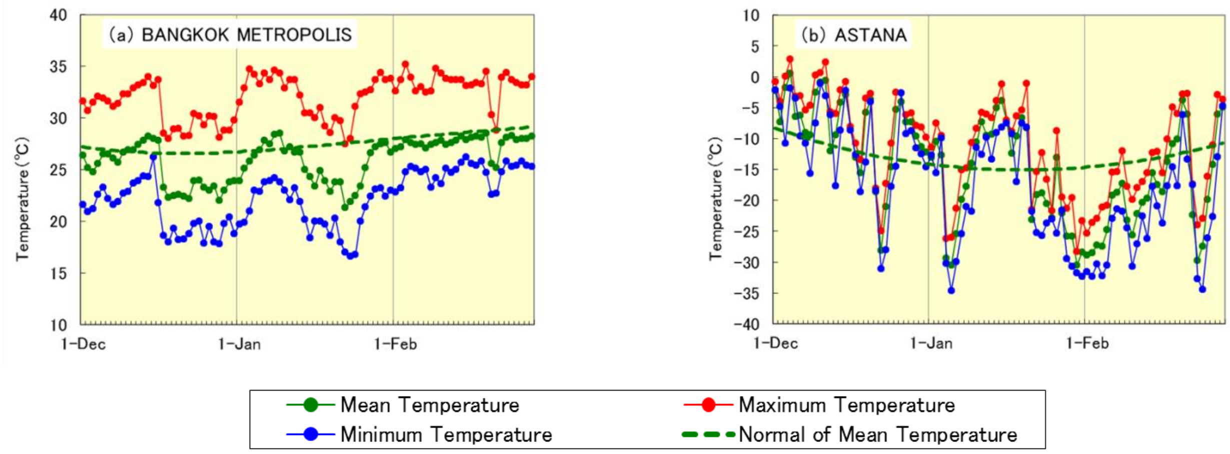

Figure 11 Time-series representation of daily maximum, mean and minimum temperatures (°C) at Bangkok in Thailand and Astana in Kazakhstan from 1 December 2013 to 28 February 2014 (based on SYNOP reports)

1.2 Heavy snowfall over northern and eastern Japan in February 2014

The Pacific side of northern and eastern Japan experienced two heavy snowfall events in February 2014. The one that occurred in mid-February had a devastating impact on socio-economic activities.

A developing low-pressure system forming on 13 February moved northeastward to the south of mainland Japan and reached the eastern part of northern Japan on 16 February. In association with this system, snow fell over a wide area mainly on the Pacific side from western to northern Japan. Some parts of the north's Tohoku region and the east's Kanto/Koshin region experienced record-breaking snowfall from 14 to 15 February. Northern Japan was also hit by heavy snowfall and severe snowstorms from 15 to 19 February.

New records for maximum snow depth were set at 18 stations in northern Japan and in the Kanto/Koshin region (for stations with statistics spanning a period of over 10 years) (Table 1 and Figure 12). In Tokyo, the maximum snow depth of 27 cm was the joint eighth highest since 1875. According to the Cabinet Office, the event in mid-February claimed 26 lives across the country and had a heavy socio-economic impact.

Table 1 Selected stations observing record snow depths on 15 February 2014

Station name (prefecture)	Maximum snow depth	Previous record (year)	Data since
Shirakawa (Fukushima)	76 cm	74 cm (1946)	1940
Utsunomiya (Tochigi)	32 cm	30 cm (1945)	1890
Maebashi (Gunma)	73 cm	37 cm (1945)	1896
Kumagaya (Saitama)	62 cm	45 cm (1936)	1896
Kofu (Yamanashi)	114 cm	49 cm (1998)	1894
Karuizawa (Nagano)	99 cm	72 cm (1998)	1925

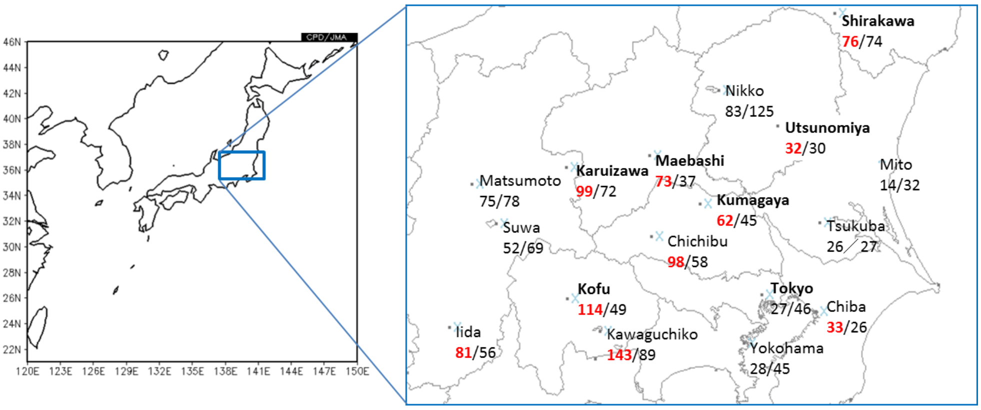

Figure 12 Maximum snow depths (cm) at selected stations in the Kanto/Koshin region

The values on the left and right indicate maximum snow depths recorded on 15 February 2014 (except Chiba, Tsukuba and Mito, whose data are from 9 February) and record-high snow depths, respectively. Values in red denote new records.

2. Characteristic atmospheric circulation and oceanographic conditions

2.1 Overview of the tropics and Southeast Asia

In winter 2013/2014, sea surface temperatures (SSTs) were above normal in the western equatorial Pacific and below normal in the central and eastern equatorial Pacific (Figure 13). SST anomalies indicated warm conditions in the South Indian Ocean and cold conditions in the North Indian Ocean and the South China Sea. Active convection areas compared to the normal gradually moved eastward from the Indian Ocean in December to the dateline region in February (Figure 14 (b)). In the western equatorial Pacific, significant westerly wind anomalies (westerly wind burst events) were seen in the second half of January and the period from the second half of February to early March (Figure 14 (c)). This activity during the latter period was associated with the Madden-Julian Oscillation (Figure 14 (a)).

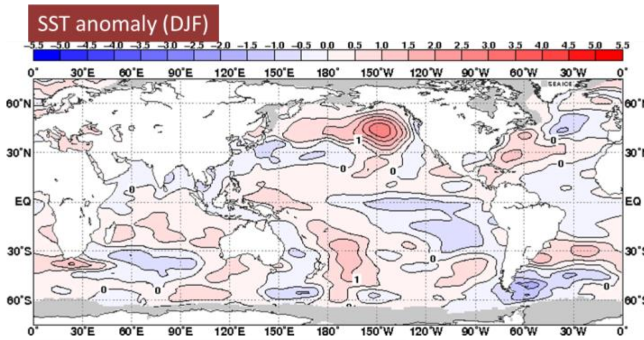

Figure 13 Three-month mean sea surface temperature (SST) anomalies for December 2013 – February 2014

The contour interval is 0.5˚C.

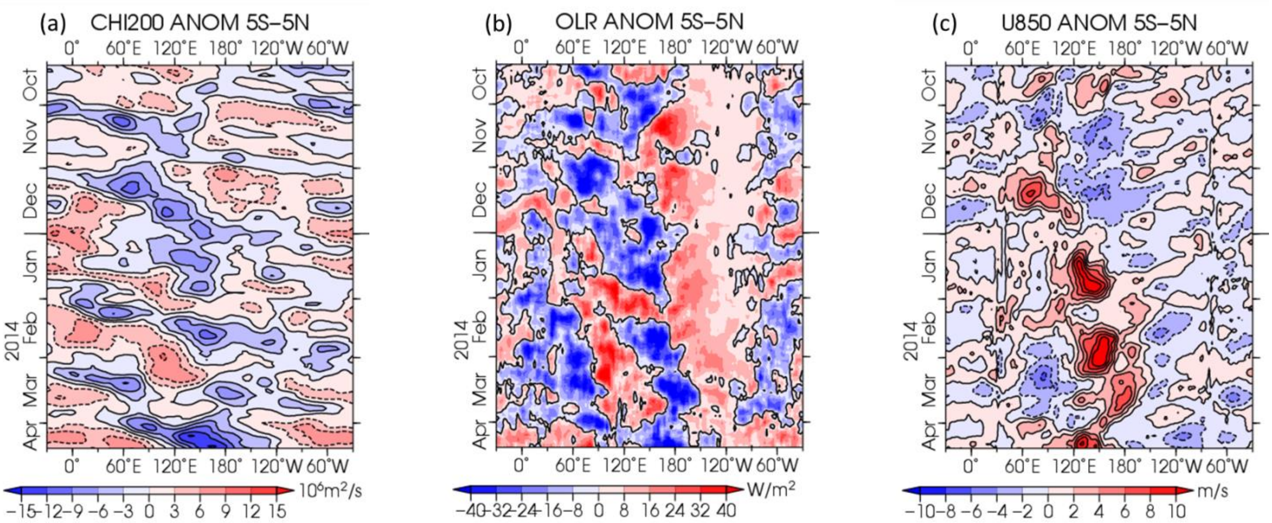

Figure 14 Time-longitude cross section of seven-day running mean (a) 200-hPa velocity potential anomalies, (b) outgoing longwave radiation (OLR) anomalies, and (c) 850-hPa zonal wind anomalies around the equator (5°S – 5°N) from mid-October 2013 to mid-April 2014

(a) The contour interval is 3×10^6 m^2/s. The blue and red shading indicates areas of divergence and convergence anomalies, respectively. (b) The blue and red shading indicates areas of enhanced and suppressed convective activity, respectively. (c) The contour interval is 2 m/s. The blue and red shading shows easterly and westerly wind anomalies, respectively.

In December 2013, large-scale divergence anomalies in the upper troposphere over the Indian Ocean and the Maritime Continent (Figure 15 (a)) indicated enhanced convective activity that contributed to heavy rainfall over parts of the Maritime Continent. Upper-level large-scale convergence anomalies were seen over the dateline region, indicating suppressed convective activity there. In the 850-hPa stream function field, cyclonic and anti-cyclonic circulation anomalies straddling the equator were observed over the Indian Ocean and the western Pacific, respectively (Figure 16 (a)), in association with the anomalous convective activity seen over the Indian Ocean and the Pacific.

In January 2014, large-scale divergence anomalies in the upper troposphere were seen over the eastern Maritime Continent and the western Pacific (Figure 15 (b)). In the lower troposphere, a pair of cyclonic circulation anomalies was centered near the Philippines and the northern coast of Australia, with northerly wind anomalies around the South China Sea and strong westerly wind anomalies over the western equatorial Pacific (Figure 16 (b)). The results of linear baroclinic model experiments forced with convective heating and cooling anomalies over the tropics show such lower-level circulation anomaly patterns and below-normal temperatures around the South China Sea (Figure 17). It can therefore be presumed that anomalous convective activity in the tropics contributed to stronger-than-normal northerly winds and extremely low temperatures over the Indochina Peninsula and the Philippines.

In February 2014, large-scale divergence anomalies in the upper troposphere were seen over the western Pacific and the dateline region, and convergence anomalies were observed over the Maritime Continent (Figure 15 (c)), contributing to dry conditions in parts of Indonesia and on the Malay Peninsula. In the lower troposphere, a pair of cyclonic circulation anomalies was seen over the western Pacific with strong westerly wind anomalies over its equatorial area (Figure 17). Such anomaly patterns were displaced eastward of those observed in January.

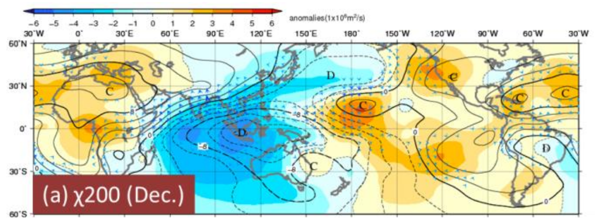

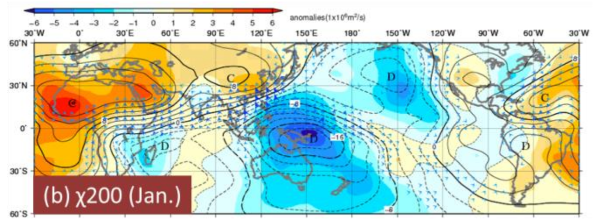

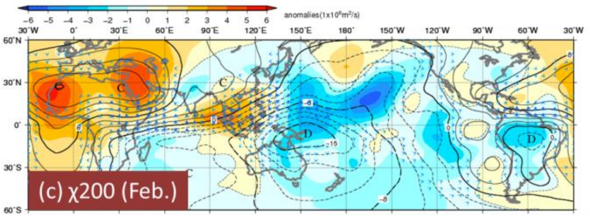

Figure 15 Monthly mean 200-hPa velocity potential for (a) December 2013, (b) January 2014 and (c) February 2014

The contours indicate velocity potential at intervals of 2×10^6 m^2/s, and the shading shows velocity potential anomalies. D and C indicate the bottom and peak of velocity potential corresponding to the centers of large-scale divergence and convergence, respectively.

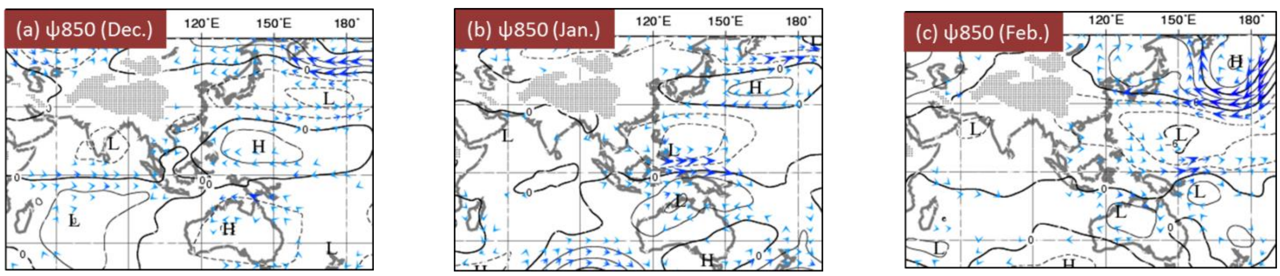

Figure 16 Monthly mean 850-hPa stream function anomalies and wind vector anomalies for (a) December 2013, (b) January 2014 and (c) February 2014

The contours indicate stream function anomalies at intervals of 2×10^6 m^2/s, and vectors show wind vector anomalies. H and L indicate the centers of anticyclonic and cyclonic circulation anomalies, respectively.

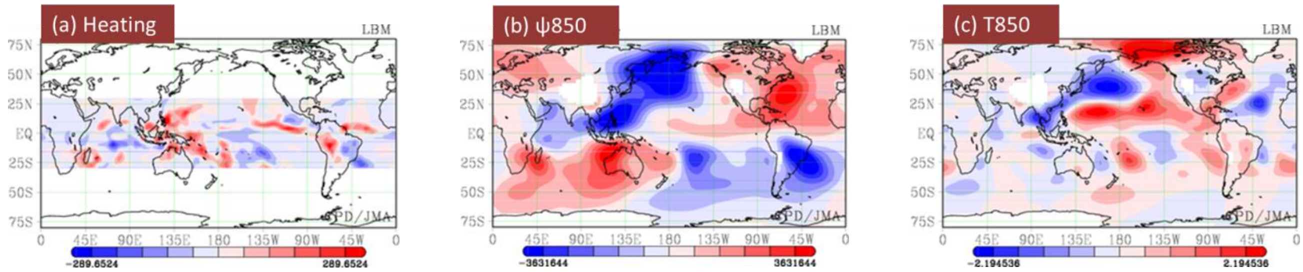

Figure 17　Steady response to heating anomalies in the tropics for January 2014 in a linear baroclinic model (LBM)
(a) The red and blue shading indicates diabatic heating and cooling, respectively, for the LBM with the basic state for January (i.e., the 1981 – 2010 average). (b) The shading denotes the steady response of 850-hPa stream function anomalies (m^2/s). (c) The shading shows the steady response of 850-hPa temperature anomalies (°C). These anomalies as responses represent deviations from the basic states, and are additionally subtracted from the zonal averages of the anomalies.

2.2 Overview of the Northern Hemisphere and East Asia

In winter 2013/2014, the polar vortex tended to be shifted toward Canada in the 500-hPa height field, and distinct troughs persisted over the central-eastern part of North America (Figure 18). In association, Arctic cold air frequently flowed over a large area of North America and caused cold conditions there, especially over the Midwest area of the USA (Figure 19). Strong low-pressure systems centered to the northwest of the UK persisted during the winter (Figure 20), contributing to significantly above-normal rainfall in the country. The intensity of the Siberian High varied significantly with a period of approximately 30 days (Figure 21 (a)), and its winter average showed normal intensity (Figure 21 (b)).

In December 2013, blocking ridges were seen over Siberia (Figure 18 (a)), contributing to extremely warm conditions there (Figure 10 (a)). In January 2014, the polar vortex was split into two in association with the development of ridges seen over the Arctic Ocean, and one of the two vortices with arctic cold air was displaced over Siberia (Figure 18 (b)), contributing to below-normal temperatures in the region (Figure 9 (b)). Zonally elongated positive anomalies were seen over East Asia, indicating that the polar-front jet stream exhibited no tendency to meander southward over the region compared to the normal. In association, China and Mongolia experienced extremely warm conditions (Figure 10 (b)). In February 2014, the polar vortex was split into two and displaced toward Canada and central Siberia, and blocking ridges developed over eastern Siberia and northwestern Russia (Figure 18 (c)). In association, temperatures were above normal in eastern Siberia and below normal in its western and central parts (Figure 19 (c)).

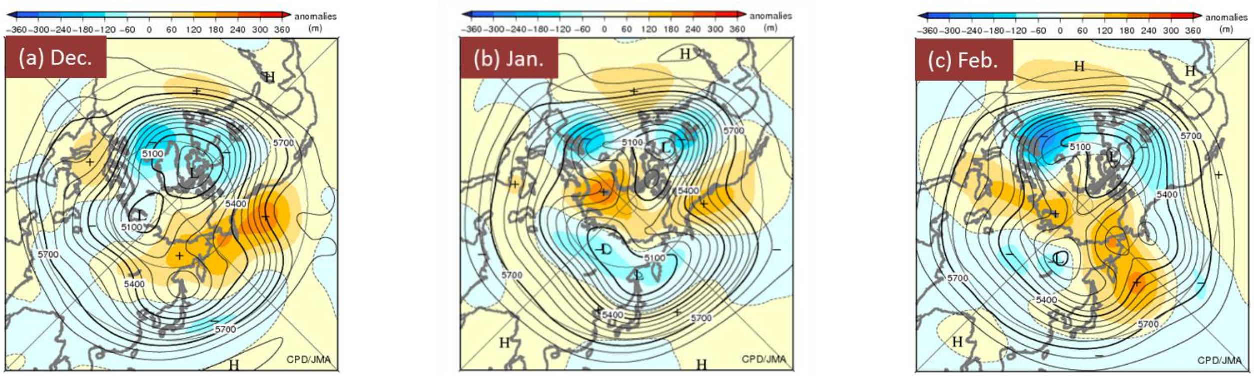

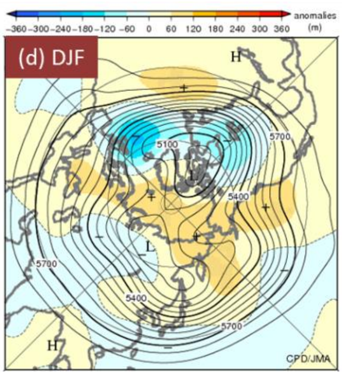

Figure 18　Monthly mean 500-hPa height for (a) December 2013, (b) January 2014 and (c) February 2014, and (d) three-month mean 500-hPa height for December 2013 – February 2014
The contours indicate 500-hPa height at intervals of 60 m, and the shading shows related anomalies. H and L indicate the peak and bottom of 500-hPa height, respectively, and + (plus) and – (minus) show the peak and bottom of related anomalies, respectively.

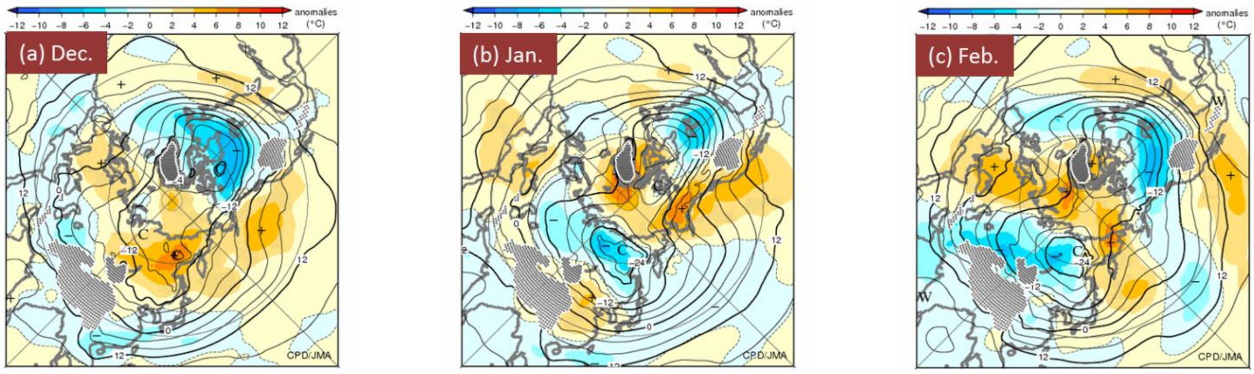

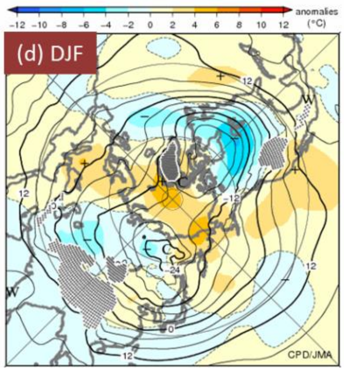

Figure 19 Monthly mean 850-hPa temperature for (a) December 2013, (b) January 2014 and (c) February 2014, and (d) three-month mean 850-hPa temperature for December 2013 – February 2014

The contours indicate 850-hPa temperature at intervals of 4°C, and the shading shows related anomalies. W and C indicate the centers of warm and cold air masses, respectively, and + (plus) and – (minus) show the peak and bottom of 850-hPa temperature anomalies, respectively.

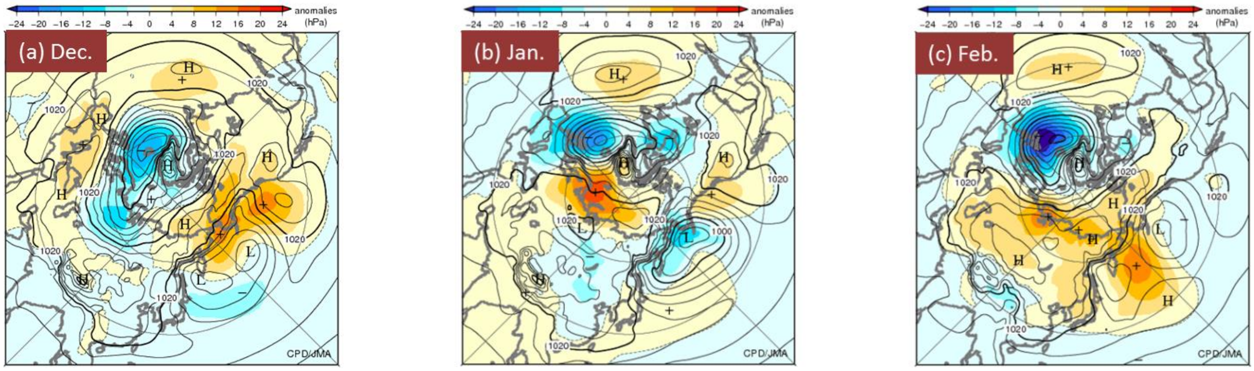

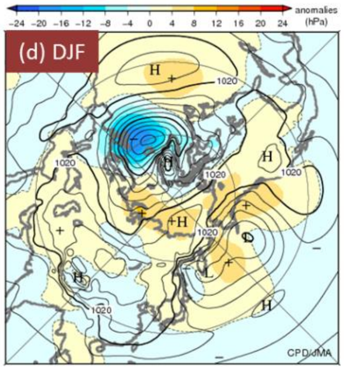

Figure 20 Monthly sea level pressure for (a) December 2013, (b) January 2014 and (c) February 2014, and (d) three-month mean sea level pressure for December 2013 – February 2014

The contours indicate sea level pressure at intervals of 4 hPa, and the shading shows related anomalies. H and L indicate the centers of high- and low-pressure systems, respectively, and + (plus) and – (minus) show the peak and bottom of sea level pressure anomalies, respectively.

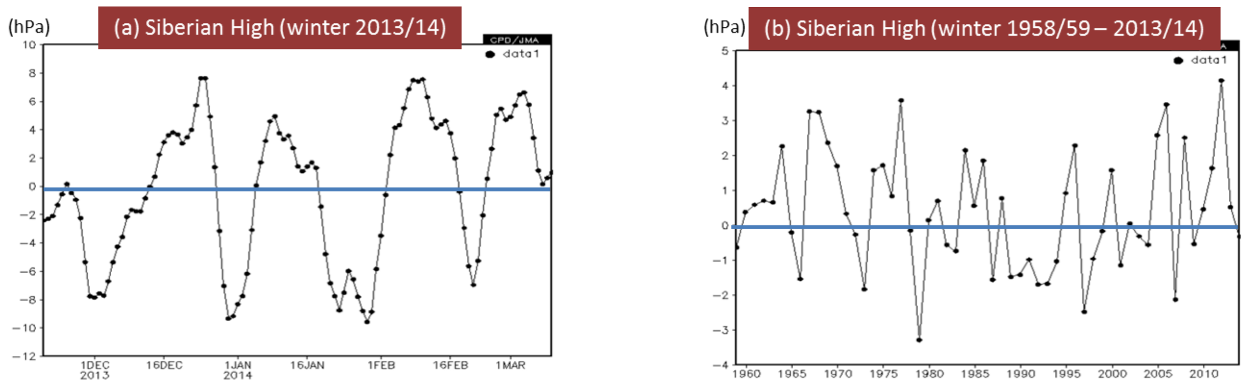

Figure 21 (a) Intraseasonal and (b) interannual variations of area-averaged sea level pressure anomalies around the center of the Siberian High (40°N – 60°N, 80°E – 120°E) for winter

(a) The black line indicates five-day running mean values for the period from 20 November 2013 to 10 March 2014. (b) The black line indicates three-month mean values for December-January-February from 1958/1959 to 2013/2014.

3. Summary

Extreme climate events were seen for relatively short periods in parts of Asia in winter 2013/2014, but none persisted widely.

(1. Ayako Takeuchi 2-3. Shotaro Tanaka, Tokyo Climate Center)

Reference

JMA, 2006: Characteristics of Global Sea Surface Temperature Data (COBE-SST), *Monthly Report on Climate System*, Separated Volume No. **12**.

New provision of Monthly Discussion on Seasonal Climate Outlooks

In its role as a WMO Regional Climate Center, the Tokyo Climate Center (TCC) provides support materials and arranges capacity development activities for National Meteorological and Hydrological Services (NMHSs) in the Asia-Pacific region to assist with their climate services, and also works to improve and develop products based on advice and requests from NMHSs (Figure 22).

On 25 March 2014, a new product called Monthly Discussion on Seasonal Climate Outlooks was launched via the TCC website (http://ds.data.jma.go.jp/tcc/tcc/products/model/index.html). Its content is intended to assist Asia-Pacific NMHSs in interpreting and assessing the products of GPC Tokyo (a Global Producing Center of Long-range Forecasts) for three-month predictions and warm/cold season forecasting. It is also designed to help NMHSs understand the current conditions of the climate system, and consists of chapters titled Summary and Discussion, Latest State of the Climate System, Three-month Predictions, Warm/Cold Season Predictions (issued in February/September), and Explanatory Notes. The product is updated around the 25th of every month. TCC welcomes comments and requests from NMHSs toward the Monthly Discussion's further improvement for use in their seasonal outlook production work.

(Shotaro Tanaka, Tokyo Climate Center)

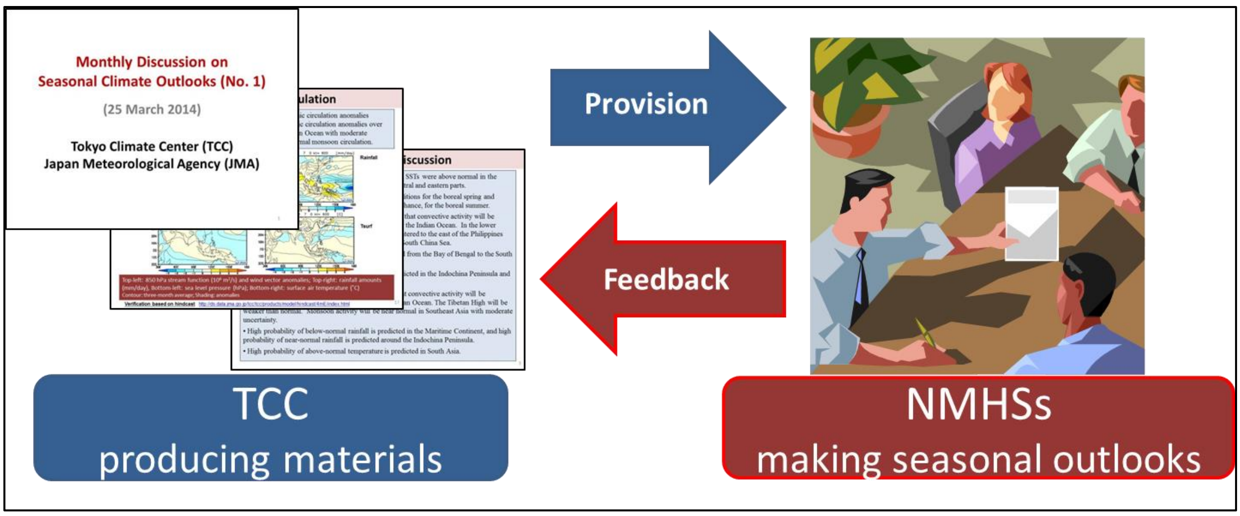

Figure 22 Support-feedback cycle involving TCC materials and NMHS seasonal outlook production

TCC expert participation in RCOFs

WMO Regional Climate Outlook Forums (RCOFs) bring together national, regional and international climate experts on an operational basis to produce regional climate outlooks based on input from participating NMHSs, regional institutions, Regional Climate Centers and global producers of climate predictions. By providing a platform for countries with similar climatological characteristics to discuss related matters, these forums ensure consistency in terms of access to and interpretation of climate information.

In April 2014, TCC experts participated in two RCOFs. These were the tenth session of the Forum on Regional Climate Monitoring, Assessment and Prediction for Regional Association II (FOCRAII) held in Beijing, China, from 23 to 25 April, and the fifth session of the South Asian Climate Outlook Forum (SASCOF-5) held in Pune, India, from 22 to 23 April. At both events, the TCC attendees gave presentations on seasonal predictions based on JMA's numerical model and participated in discussions to produce consensus forecasts.

(Ryuji Yamada, Tokyo Climate Center)

Launch of website for the Pilot Project on Information Sharing on Climate Services

The Global Framework for Climate Services (GFCS) is one of WMO's current top-five priorities. For its successful implementation, it is important to share good practices and lessons learned, including information on experienced project management capabilities, toward the development of projects and the improvement of climate services run by NMHSs. There is also a need to avoid duplication of work and minimize the risk of failure.

At its 15th session (December 2012, Doha, Qatar), WMO Regional Association II decided to establish a pilot project for the sharing of information on climate services. The initiative is intended to support such sharing and the transfer of information on best practices regarding climate information among NMHSs in the region through a dedicated website toward the successful implementation of GFCS work.

In its designated lead role on the project, the Tokyo Climate Center (TCC) developed and distributed a project questionnaire to nominated focal points in order to collect relevant information. Based on the responses, staff from the Center worked on the development of a portal site that was launched in March 2014 on the TCC website at http://ds.data.jma.go.jp/tcc/pilot/. The portal features individual RA II Member web pages, and each page has links to climate information, data and products (including long-range forecasting and climate monitoring) provided by the NMHSs concerned. TCC will continue to collect pertinent information from NMHSs to be shared with Members. The website is expected to support the consideration of future work to facilitate the utilization of climate information.

(Ryuji Yamada, Tokyo Climate Center)

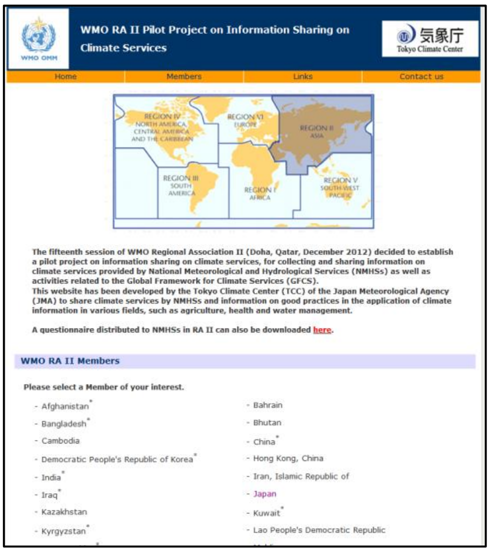

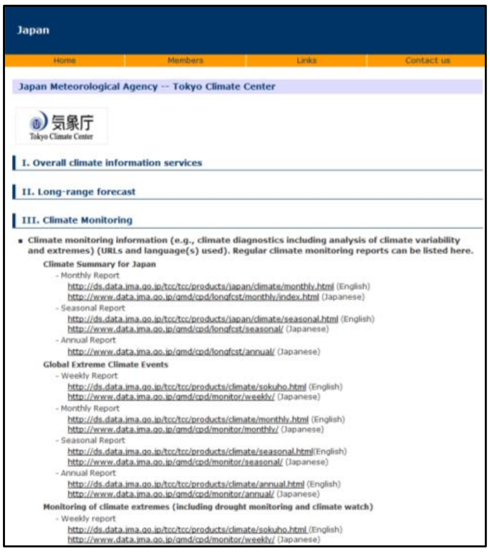

Any comments or inquiry on this newsletter and/or the TCC website would be much appreciated. Please e-mail to tcc@met.kishou.go.jp.
(Editors: Teruko Manabe, Ryuji Yamada and Yasushi Mochizuki)

Tokyo Climate Center (TCC), Japan Meteorological Agency
Address: 1-3-4 Otemachi, Chiyoda-ku, Tokyo 100-8122, Japan
TCC Website: http://ds.data.jma.go.jp/tcc/tcc/index.html